Electronic Supplementary Material (ESI) for Nanoscale.

Supplementary Information

Revealing the Role of Catechol Moieties in the Interactions between Peptides and Inorganic Surfaces

*Priyadip Das and Meital Reches**

Institute of Chemistry and The Center for Nanoscience and Nanotechnology, The Hebrew University of Jerusalem, 91904 Jerusalem, Israel.

* Email: *meital.reches@mail.huji.ac.il*

Surface preparation and characterization

A silicon wafer (100) was cut into squares of 2 cm^2 using a diamond pen. The substrates were then cleaned in acetone followed by isopropanol in an ultrasonic bath. To prepare the TiO_2 coated substrate we used wet deposition technique. [1] At first 0.02 ml of ByK^{348}, a wetting agent (5% prepared in ethanol) was added to a 2 ml solution of 30% TiO_2 dispersion (TiO_2 nanoparticles (20-25 nm) dispersion (30%) in the mixture of solvent 2-(2-Methoxyethoxy) ethanol (DEGME) and Ethyl 3-Ethoxypropionate (EEP) (commercially available for coating). The resulting solution drop cast on a clean silicon wafer and bar coated to make the drop casting uniform over the surface. The last step included annealing at 250˚C for two hours in air. We characterized this resulting TiO_2-coated surface by AFM, X-ray diffraction (XRD), and contact angle measurement.

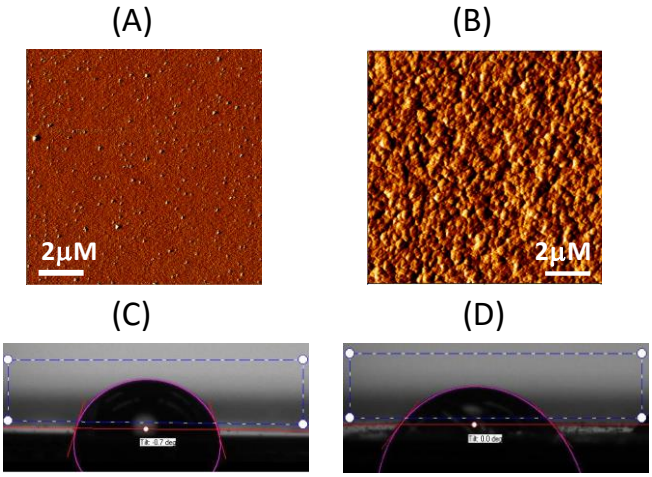

Figure S1. Representative AFM micrographs of the (A) bare Si surface and (B) the TiO_2-coated Si surface. Contact angle measurement of (C) the bare Si surface (73°) and (D) the TiO_2-coated Si surface (49°). (E) The X-ray diffraction pattern of the bare Si surface (blue) and the TiO_2-coated Si surface (red).

XRD analysis for the bare Si and TiO_2 coted Si surface

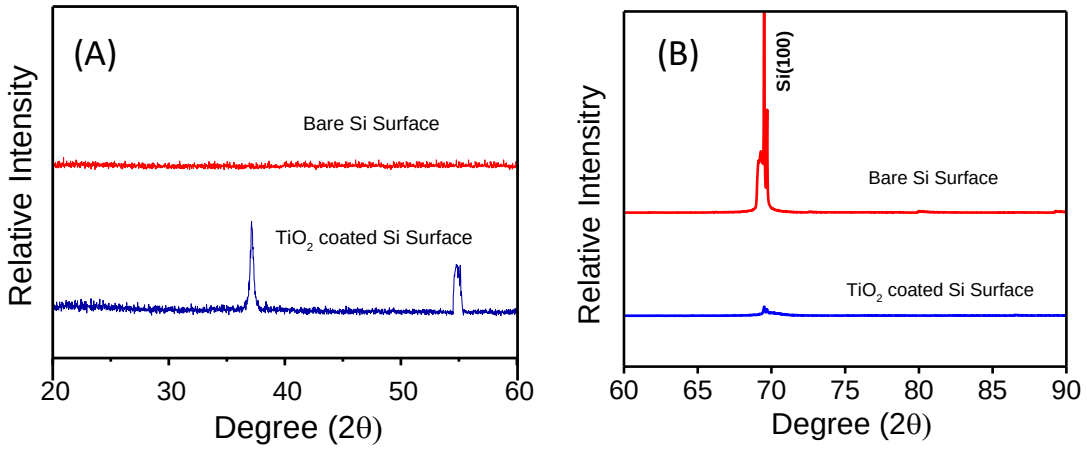

Figure S2. (A) The X-ray diffraction pattern of the bare Si surface (red) and the TiO_2-coated Si surface (blue) in the 2θ region 20°-60° (B) The X-ray diffraction pattern of the bare Si surface (red) and the TiO_2-coated Si surface (blue) in the 2θ region 60°-90°.

The topography analysis (Figure 1A and 1B) clearly revealed that the TiO_2 nanoparticles were nicely adsorbed on the bare Si surface and formed a TiO_2 layer. The contact angle of the coated surface decreased from 73°, for a bare silicon surface, to 49° for a TiO_2 substrate, which indicates a more hydrophilic surface. The reactivity of the TiO_2 surface and in particular, its affinity toward water depends on the TiO_2 crystal phase.[2-3] In this context, Bolis et al. described the hydrophilic or hydrophobic character of the TiO_2 surface as a function of a crystal phase, surface area, and the nature of the coating.[4] The interaction of the TiO_2 surface with water depends on the particular ‘‘form’’ of the considered material, including the abundance of defects present on non-stoichiometric reduced surfaces. [5] We further analyzed the TiO_2-coated and bare Si surface using XRD. The XRD spectrum of the TiO_2-coated surface exhibited two peaks in the range of 2θ (20°-60°) at ~37° and ~55° (Figure S2 A), which characterize the rutile crystal phase.[6] The crystallite size obtained from the XRD analysis of the TiO_2-coated surface was 31.8 nm and further suggested the rutile phase.[4] The bare Si surface showed a high intensity of the characteristic peak (~ 70° for Si (100)) while the TiO_2 coated surface only had a peak with negligible intensity for (Figure S2B). This suggests a consistent and uniform coating of TiO_2 over the silicon surface.

X-ray photoelectron spectroscopy (XPS)

The X-ray Photoelectron Spectroscopy (XPS) measurements were performed using a Kratos Axis Ultra X-ray photoelectron spectrometer (Karatos Analytical Ltd., Manchester, UK) using an Al Kα monochromatic radiation source (1,486.7 eV) with a 90° takeoff angle (normal to analyzer). The high-resolution XPS spectra were collected for C 1s, B 1s, F 1s, O 1s, and Si 2p levels with a pass energy of 20 eV and a step size of 0.1 eV. The binding energies were calibrated relative to the C 1s peak energy position as 285.0 eV when needed. Data analyses were performed using Casa XPS (Casa Software Ltd.) and a Vision data processing program (Kratos Analytical Ltd.).

Contact angle measurements

Contact angle measurements were carried out using a Theta Lite optical tensiometer (Attension, Finland).

Tip Characterization

We chemically modified SiN_4 cantilevers with Si tips having a nominal radius of ~ 2nm to examine the interaction between single amino acid residues and TiO_2- coated surfaces. The chemical modification of the Si tips was done based on our previous report (scheme 1).[7] At first, we functionalized the plasma-treated tip with a layer of two silane compounds: methyltriehoxysilane (MTES) and 3-(aminopropyl) triehoxysilane (APTES). These free amine groups help to attach the flexible linker poly (ethylene glycol) (PEG), which is a soft molecule with nonlinear elasticity that allows us to differentiate between non-specific interaction with the tip only and the specific interaction of the attached molecule with the desired surface. In our method we used Fmoc-PEG-NHS, which has a protected amine group at its terminus. Finally, the desired N-Boc-protected amino acid residue was attached to the tip by coupling with the free amine group of the PEG molecule (scheme 1).

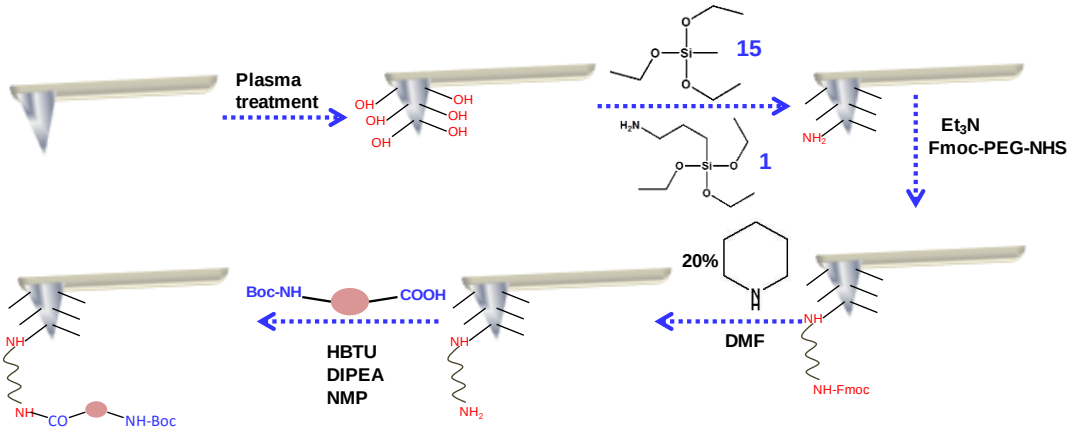

Scheme 1. Schematic representation of the chemically modified procedure of the AFM tip.

In order to ensure that the chemical modification of the tip was successful, we modified/functionalized a silicon (100) substrate with penta fluoro phenyl alanine following the same procedure employed for the chemical modification of the AFM tip. The resulting surface was characterized at different steps of the modification procedure using the XPS technique. Figure 2A shows the difference in the Si (2p) intensity signal at different stages of chemical modification.

Furthermore, from the XPS analysis we also monitored the existence F (1s) signal only after completely modifying the Si surface with fluorinated phenylalanine. This signal is also absent when a clean Si surface is deposited in a solution of fluorinated phenylalanine. This result confirms that the amino acid residue is attached to the Si tip, using this chemical modification procedure.

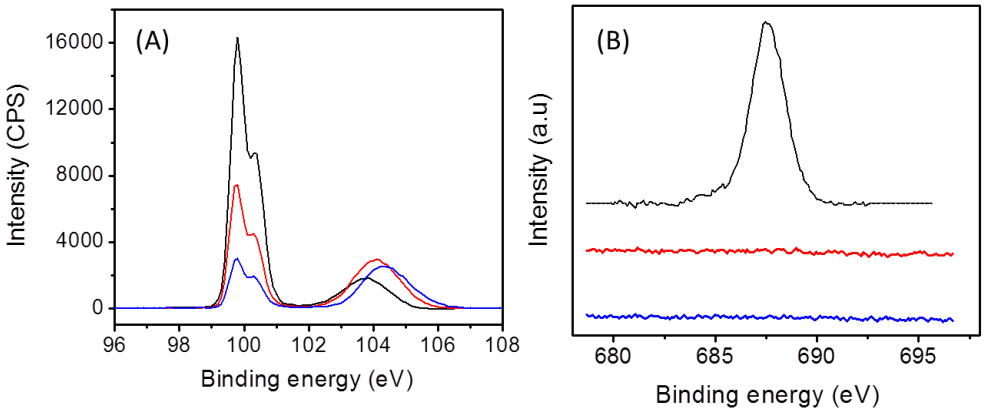

Figure S3. XPS analysis of a Si substrate at different stages of the chemical modifications. (A) Silicon signal (Si 2p level) obtained during the modification with fluorinated phenylalanine. The black line represents a bare, cleaned silicon surface; the red line, the surface after PEGylation; and the blue line, a surface modified with fluorinated phenylalanine

after complete modification. The reduction in the intensity of the signal after each step indicates the layers added on the silicon. (B) Fluorine atom signal (1s level) at different stages of chemical modification. The blue line represents a clean silicon surface; the red line, a surface after PEGlyation; and the black line, a surface completely modified with the fluorinated amino acid.

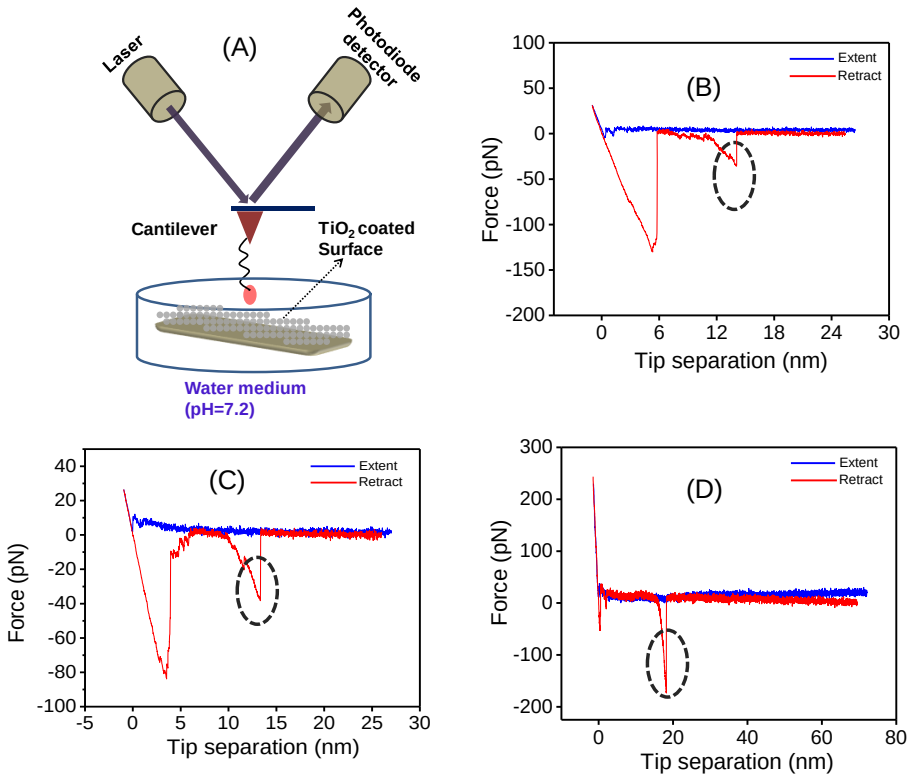

Figure S4. (A) Schematic illustration of SMFS experiments involving different amino acids with TiO2-coated surfaces. Typical single-molecule F-D curves for the rupture of different examined amino acids (B) Phenylalanine, (C) Tyrosine, and (D) dopamine with TiO2-coated surfaces in aqueous-buffer medium (pH =7.2). The blue and red traces indicate approach and retraction signals, respectively. Each peak marked with a black dashed circle corresponds to the unbinding force of the specific single-molecule adhesion event of the amino acids with a TiO_2-coated surface.

Estimation of thermodynamic and kinetic parameters through the Bell–Evans approach:

In order to obtain more information on the binding nature of these examined amino acid residues, we employed the Bell-Evans model.[8-9] This model provides the logarithmic dependence of the MPF with the apparent loading rate through the following equation:

$$F = \frac{k_B T}{x_b} \ln\left(\frac{x_b}{K_{Off} k_B T}\right) + \frac{k_B T}{x_b} \ln\ (r)$$

Using this linear dependency, we quantified the distance of the transition state or rupture distance (x_b) and the dissociation rate at equilibrium (K_{Off}), where F is the most probable rupture force, k_B is the Boltzmann constant, and T is the absolute temperature. Furthermore, the free energy barrier for the unbinding or bond dissociation energy (ΔG) can be calculated using the following equation:

$$\Delta G = -k_B T\ ln\ \left(\frac{K_{Off}}{\nu}\right),$$

where ν is the Arrhenius prefactor or the frequency factor (we chose A of $\approx 10^6\ S^{-1}$ in our calculation).[10] The MPF value calculated for several loading rates (r) was plotted as a function of ln *(r)* (Figure 4D-F). The equilibrium parameters x_b and K_{Off} were obtained from the values of the slope and the intercept of the linear plot, respectively (**Figure 2D-F**) and ΔG was derived from the value of K_{Off}. All the kinetic parameters evaluated for all three amino acids (Phe, Tyr, DOPA) are summarized in table 1.

Estimation of Bond Dissociation Energy for dopa-quinone (in basic medium pH =9.8) on TiO_2:

The bond dissociation energy was calculated from the pulling rate dependence of the pull-off force, as described by Evans and coworkers .[9] The relationship between force (F) and the loading rate (r) is given by

$$F = \frac{k_B T}{x_b} \ln\left(\frac{x_b}{K_{Off} k_B T}\right) + \frac{k_B T}{x_b} \ln\ (r) \quad \text{..... (1)}$$

Where x_b is the rupture distance, $k_B T$ is the thermal energy, K_{Off} is the dissociation rate at equilibrium. Furthermore, the free energy barrier for the unbinding or bond dissociation energy (ΔG) can be calculated using the following equation:

$$\Delta G = -k_B T\ ln\ \left(\frac{K_{Off}}{\nu}\right) \quad \text{..... (2)}$$

Where ν is the Arrhenius prefactor or the frequency factor ($\approx 10^6$ s^{-1}) and ΔG is the bond dissociation energy.

Eq. **1** is linear; a plot of F vs. ln(r) would have a slope of $\frac{k_B T}{x_b}$. Considering the similar value for the bond length (x_b), which was obtained for the unoxidized DOPA–TiO_2 interaction (1.15 Å)), yields a slope $\left(\frac{k_B T}{x_b}\right)$ = 3.57 X 10^{-11} J/m.

Based on the calculated slope and the experimentally measured dopa–quinone–TiO_2 force

[108 pN at ln(r) = 8. 489 from Fig. 3*B*], the *y*-intercept is estimated to be -195.057 pN. K_{Off} is then determined from equation 3,

$$\text{-195.057} = \frac{k_B T}{x_b} \ln\left(\frac{x_b}{K_{Off} k_B T}\right) \quad \text{..... (3)}$$

The value of K_{Off} is 6.35S^{-1}, Finally, using Eq. **2**, the bond dissociation energy for dopa–quinone–TiO_2 was estimated to be 29.54 kJ/mol

Estimation of most probable force for the interaction of DOPA-Si and DOPA -SiO_2

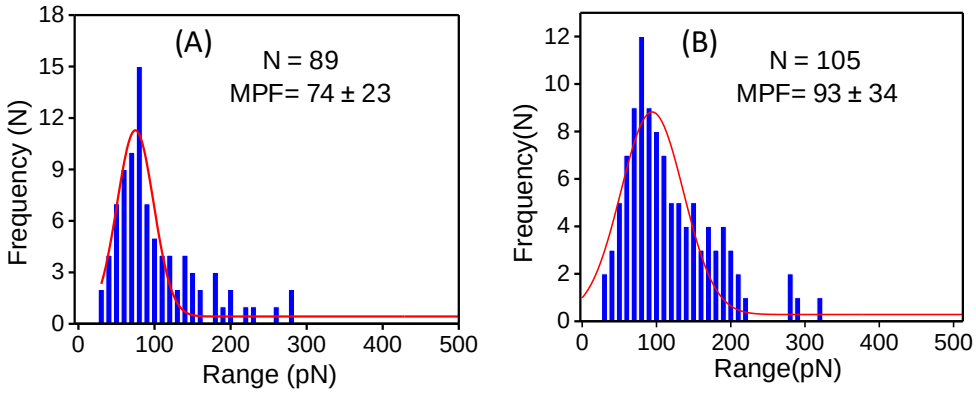

Figure S5. Histograms of the rupture force values for (A) DOPA-bare Si, (B) DOPA-SiO_2 interaction (loading rate of 4.38 ± 0.7 nN s^{-1}, 4.62 ± 0.5 nN s^{-1}, respectively in Tris buffer (50 mM, pH=7.2)).

References

1. S. Azoubel and S. Magdassi, *ACS Appl. Mater. Interfaces.*,, 2014, **6**, 9265.
2. U. Aschauer, Y. He, H. Cheng, S.-C. Li, U. Diebold and A. Selloni, *J. Phys. Chem. C.*, 2010, **114**, 1278.
3. H. Cheng and A. Selloni, *Langmuir*, 2010, **26**, 11518.
4. V. Bolis, C. Busco, M. Ciarletta, C. Distasi, J. Erriquez, I. Fenoglio, S. Livraghi and S. Morel, *J. Colloid. Interf. Sci.*, 2012, **369**, 28.
5. A. Selloni, A. Vittadini and M. Grätzel, *Surf. Sci.*, 1998, **402–404**, 219.
6. M. Addamo, M. Bellardita, A. Di Paola and L. Palmisano, *Chem. Commun.*, 2006, 4943.
7. S. Maity, D. Zanuy, Y. Razvag, P. Das, C. Aleman and M. Reches, *Phys. Chem. Chem. Phys.*, 2015, **17**, 15305.
8. G. Bell, *Science*, 1978, **200**, 618.
9. E. Evans and K. Ritchie, *Biophys. J.*, 1999, **76**, 2439.
10. Y. Li, M. Qin, Y. Li, Y. Cao and W. Wang, *Langmuir*, 2014, **30**, 4358.